Numerical study of a mixed Ising ferrimagnetic system

1997 J. Phys.: Condens. Matter 9 5951

(http://iopscience.iop.org/0953-8984/9/27/021)

J. Phys.: Condens. Matter **9** (1997) 5951–5964. Printed in the UK PII: S0953-8984(97)80467-5

Numerical study of a mixed Ising ferrimagnetic system

G M Buendía† and M A Novotny‡

† Supercomputer Computations Research Institute, Florida State University, Tallahassee, FL 32306-4052, USA, and Departamento de Física, Universidad Simón Bolívar, Apartado 89000, Caracas 1080, Venezuela§

‡ Supercomputer Computations Research Institute, Florida State University, Tallahassee, FL 32306-4052, USA, and Department of Electrical Engineering, 2525 Pottsdamer Street, Florida A&M University, Florida State University, Tallahassee, FL 32310-6046, USA

Received 23 December 1996, in final form 25 April 1997

Abstract. We present a study of a classical ferrimagnetic model on a square lattice in which the two interpenetrating square sublattices have spins one-half and one. This model is relevant for understanding bimetallic molecular ferrimagnets that are currently being synthesized by several experimental groups. We perform exact ground-state calculations for the model, and employ Monte Carlo and numerical transfer-matrix techniques to obtain the finite-temperature phase diagram for both the transition and compensation temperatures. When only nearest-neighbour interactions are included, our non-perturbative results indicate no compensation point or tricritical point at finite temperature, which contradicts earlier results obtained with mean-field analysis.

1. Introduction

Stable, crystalline room-temperature magnets with spontaneous moments are the subject of a great deal of interest because of their potential applications, including those in areas such as thermomagnetic recording and in devices [1]. It is widely believed that ferrimagnetic ordering plays a fundamental role in some of these materials, and the synthesis of new ferrimagnetic materials is an active field in materials science.

In a ferrimagnetic material two inequivalent moments interacting antiferromagnetically can achieve a spontaneous magnetization at temperatures that are low compared with the strength of the interaction. At these low temperatures, the inequivalent moments are antiparallel but do not cancel [2, 3]. The simplest bipartite lattice to consider is a linear chain, where the sum of the moments in each unit cell can result in a large moment for the chain. If adjacent chains can be positioned such that their moments are parallel, then a transition can occur at low temperatures to a state of three-dimensional (3-D) ferrimagnetic order [4].

Important advances have been made by several groups in the synthesis of ferrimagnetic chains [5, 6]. However, it is difficult to achieve high critical temperatures with quasi-one-dimensional materials. Consequently the discovery of bimetallic molecular materials with spontaneous moments at temperatures as high as 43 K [7] has directed the experimentalist toward the formation of 2-D and 3-D bimetallic lattices [8].

Synthesis of single-chain and double-chain ferrimagnets is now becoming standard, and attempts to synthesize higher-dimensional polymeric ferrimagnets are starting to

§ Permanent address.

0953-8984/97/275951+14$19.50

give very encouraging results. Some of the materials currently under investigation are 2-D organometallic ferrimagnets [7], 2-D networks of the mixed-metal material $\{[P(Ph)_4][MnCr(ox)_3]\}_n$ where Ph is phenyl and ox is oxalate [9], 3-D ferrimagnets with critical temperatures up to 240 K [10], and the recently developed amorphous $V(TCNE)_x \cdot y$(solvent) with ordering temperatures as high as 400 K [11]. Experimental studies on recently synthesized compounds such as $N(n\text{-}C_nH_{2n+1})_4Fe^{II}Fe^{III}(C_2O_4)_3$ with $n = 3$–5 have found critical temperatures between 35 and 48 K, and some of these compounds exhibit a compensation point near 30 K [12].

The intense activity related to the synthesis of ferrimagnetic materials requires a parallel effort in the theoretical study of these materials. Mixed Ising systems provide good models for studying ferrimagnetism. The magnetic properties of these model systems have been examined by high-temperature series expansions [13], and renormalization-group [14, 15], mean-field [16] and effective-field approaches [17, 18]. A diluted mixed Ising model has also been studied using the effective-field approach [19]. An exact solution of a mixed Ising model on a Union Jack lattice has recently been found for a low-dimensional manifold in the parameter space [20]. The model on the Union Jack lattice used by the authors of [20] is equivalent to the model studied here, and their exact results are only for a two-dimensional manifold in our four-dimensional parameter and temperature space. In our work we study a classical model of a ferrimagnetic system: a mixed spin-1/2 and spin-1 system on a square lattice. We are interested particularly in the phase diagram and in the location and characterization of the compensation point: the one temperature where the resultant magnetization vanishes below the critical point (type N in the Néel classification [2]).

The behaviour at the compensation point is of fundamental significance in the field of thermomagnetic recording. It has been found that the coercivity diverges at the compensation point [21]; at this point only a small driving field is required to reverse the sign of the magnetization. Just below the compensation temperature the coercivity falls to a minimum before rising again at low temperature. This temperature dependence of the coercivity near the compensation point can be applied to writing and erasing in high-density magneto-optical recording media. The thermomagnetic effects are achieved by local heating by a focused laser beam. It has been shown that by using films with compensation temperatures higher than room temperature, it is possible to attain a direct overwrite capability in magneto-optic thin films [22].

In section 2 we present the Hamiltonian of the model and its ground states. We next briefly describe the non-perturbative techniques used to study the model: Monte Carlo (section 3) and numerical transfer-matrix calculations (section 4). In section 5 we discuss our results, and finally we present the conclusions of our work in section 6. Preliminary results for our model have been published elsewhere [23].

2. The model and its ground states

Our model consists of spins on two interpenetrating square sublattices. One sublattice has spins σ on the lattice sites, where σ has two states, $\sigma = \pm 1$. The spins σ are spin 1/2, but we choose to put the factor of 1/2 into the interaction parameters. The sites of the other sublattice have spins S which can have three states, $S = \pm 1, 0$. Each spin σ has only S-spins as nearest neighbours, and vice versa. The Hamiltonian that we study is

$$\mathcal{H} = -J_1 \sum_{\langle \mathrm{nn} \rangle} \sigma_i S_j - J_4 \sum_{\langle \mathrm{nnn} \rangle} \sigma_i \sigma_k + D \sum_j S_j^2 \tag{1}$$

where the sums $\sum_{\langle nn\rangle}$ and $\sum_{\langle nnn\rangle}$ are over all of the nearest-neighbour (nn) and next-nearest-neighbour (nnn) bonds, respectively. Each J is an exchange interaction parameter, and D is the crystal field, all in energy units.

We fix J_1 to be negative, so the coupling between the nn spins is antiferromagnetic. It is well known that the model with $J_4 = D = 0$ does not have a tricritical point [24]. However, recent studies based on mean- and effective-field theories indicate that the crystal field D plays an important role in the magnetic behaviour of the system, and that the $J_4 = 0$ model has interesting characteristics such as tricritical and compensation points [16, 18, 19]. Since using mean-field theories is a very approximate way to study Ising models, and in view of the fact that the compensation point has technological significance and is being measured in the new synthesized ferrimagnetic materials, we consider it important to test the magnetic behaviour of these models using non-perturbative techniques. Monte Carlo and numerical transfer-matrix methods have proven to be efficient and accurate methods for studying Ising and a great variety of other models.

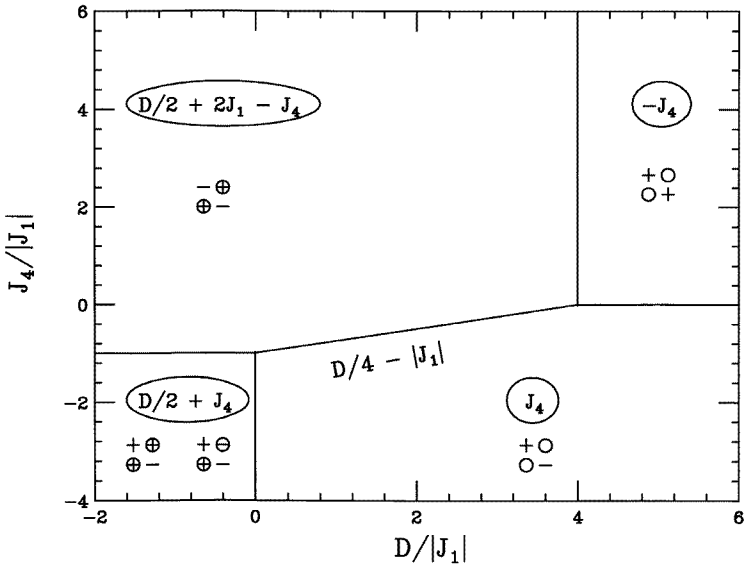

Figure 1. The ground-state diagram for the model. There are four regions, in each of which the configurations of the 2×2 cells are indicated. The spins S are enclosed in circles, and may be ± 1 or 0. The transition line not parallel to the coordinate axes is labelled by the right-hand side of the defining equation, $J_4 = aD + b|J_1|$. Inside the ellipses are the energies per site of the 2×2 cell.

In order to find the ground-state diagram for finite values of the parameters, we use a 2×2 cell. For our Hamiltonian the ground state is translationally invariant, and a 2×2 cell is sufficient for including all possible ground states [25]. With rotational symmetry taken into account, the 2×2 cell has $2^2 3^2/2 = 18$ configurations. Figure 1 shows the ground-state diagram for the Hamiltonian in equation (1) for $J_1 < 0$, where the boundaries between the regions are obtained by pairwise equating of the ground-state energies. The critical values of the parameters at which the zero-temperature phase transitions occur are shown in the graphs. When performing non-perturbative studies at finite temperature, we will pay special attention to the vicinities of these points.

3. Monte Carlo calculations

Standard importance-sampling methods [26] were applied to simulate the model described by the Hamiltonian of equation (1) on square lattices of $L \times L$ sites with periodic boundary conditions. Most of the data were obtained with $L = 40$, but we also present some results for $L = 10$, $L = 16$, and $L = 60$. Configurations were generated by sequentially traversing the lattice and making single spin-flip attempts. The flips were accepted or rejected with standard heat-bath dynamics. We use the very-long-period (of the order of 2^{95}), random-number generator KISS (for Keep It Simple, Stupid) [27]. Data were generated with 25 000 Monte Carlo steps per site after discarding the first 2500 steps. The error bars were taken from the standard deviation of blocks of 500 measurements each. We define $\beta = 1/k_{\mathrm{B}}T$, and take the Boltzmann's constant $k_{\mathrm{B}} = 1$. Our program calculates the internal energy, the specific heat, the sublattice magnetizations M_1 and M_2 defined as

$$M_1 = \frac{2}{L^2}\left\langle \sum_j S_j \right\rangle \tag{2}$$

$$M_2 = \frac{2}{L^2}\left\langle \sum_i \sigma_i \right\rangle \tag{3}$$

and the total magnetization $M = (1/2)(M_1 + gM_2)$, where the factor $1/2$ gives the correct normalization for the whole lattice since M_1 and M_2 are normalized for the sublattice. Throughout this paper we take the g-factor to be $g = 1/2$. We also measured the order parameters

$$O_{\pm} = \frac{1}{L^2}\left\langle \left| \sum_i S_i \pm g \sum_j \sigma_j \right| \right\rangle \tag{4}$$

and the susceptibilities associated with M, M_1, M_2, and $O_{\pm}$. The averages are taken over all configurations generated, the sums over i are over all of the sites with σ-spins, and the sums over j are over all of the sites with S-spins. There are $L^2/2$ terms in each sum. We verified that our results are in agreement with exact enumeration studies for $L = 2$, and that the ground-state diagrams are reproduced for different combinations of the parameters in the Hamiltonian.

For an infinite lattice, the order parameter O_+ would not be defined with the absolute value in equation (4), and would change sign at the compensation temperature T_{comp}. However, for a finite lattice the absolute values are required to keep the order parameters non-zero in the limit of a long measurement time. An efficient way to locate T_{comp} using the Monte Carlo data is to find the crossing point of the absolute values of the sublattice magnetizations, i.e.,

$$|M_1(T_{\mathrm{comp}})| = g|M_2(T_{\mathrm{comp}})| \tag{5}$$

with the conditions

$$\mathrm{sign}(M_1(T_{\mathrm{comp}})) = -\mathrm{sign}(M_2(T_{\mathrm{comp}})) \qquad \text{and} \qquad T_{\mathrm{comp}} < T_{\mathrm{c}}. \tag{6}$$

These relations ensure that $O_+(T_{\mathrm{comp}})$ as defined in equation (4) is equal to zero.

4. Transfer-matrix calculations

Traditional numerical transfer-matrix (TM) calculations [28] were performed as a second non-perturbative method to obtain finite-temperature phase diagrams, critical exponents, and

compensation temperatures. These results were compared with the Monte Carlo results, as well as with previous mean-field calculations.

For a square lattice with different spins on each of the two square sublattices, care should be taken to ensure that the TM is symmetric. A symmetric TM is preferred, since it is much easier numerically to calculate its eigenvalues and eigenvectors. We used two different TM constructions, both of which give symmetric transfer matrices, as detailed below. The largest eigenvalues and eigenvectors of these symmetric transfer matrices were then calculated using the NAG subroutine F02FJE. This subroutine requires only multiplication of an arbitrary vector by the TM, and consequently it is not necessary to store the entire TM in memory. This allows us to use very large transfer matrices in our calculations. For both TM implementations, the lattice is wrapped on a torus of finite width and infinite extent, and periodic boundary conditions are imposed. However, the periodic boundary conditions are for a given column of spins, and lead to different boundary conditions in terms of the primitive lattice vectors, since the infinite direction of the torus may not be along a direction given by a single primitive lattice vector.

The two different implementations of the transfer matrix are called TM1 and TM2, and the details of the construction of the transfer matrices are given in the appendix. The remainder of the equations in this section are stated for the TM1 implementation with N, but would be equally valid for the TM2 implementation with N replaced by $\widetilde{N}$. The inverse correlation length, ξ_N^{-1}, is given by the ratio of the largest and next-largest eigenvalues of the TM as

$$\xi_N^{-1} = \ln\left|\frac{\lambda_1}{\lambda_2}\right|. \tag{7}$$

The scaling form for ξ is [28]

$$\xi_N = N\mathcal{F}(tN^{y_T}) \tag{8}$$

where $t = |(T - T_c)/T_c|$ is the reduced temperature. At $t = 0$, equation (8) allows one to calculate the finite-strip estimates for the critical temperature T_c as the temperature where the phenomenological scaling relation

$$\frac{\xi_N}{N} = \frac{\xi_{N+1}}{N+1} \tag{9}$$

holds. Differentiating the scaling relation given as equation (8), and evaluating it at the estimated value of T_c given by equation (9) gives the finite-strip estimate of the critical exponent $y_T = 1/\nu$ as [28]

$$y_T + 1 = \frac{\ln[(\mathrm{d}\xi_N/\mathrm{d}t|_{t=0})/(\mathrm{d}\xi_{N+1}/\mathrm{d}t|_{t=0})]}{\ln[N/(N+1)]}. \tag{10}$$

The differentiation in equation (10) was performed as a two-point finite difference.

The TM calculation of the compensation point was only done in the implementation TM2, since with $J_4 \neq 0$ the TM1 implementation is not symmetric. The standard method of calculating the magnetization by diagonalizing a 2×2 matrix formed from the expectation values of the magnetization operator using the two largest eigenvectors was used [29]. If $\boldsymbol{M}$ is the magnetization operator, the solution of the equation

$$\det\begin{vmatrix} \langle 1|\boldsymbol{M}|1\rangle - m & \langle 1|\boldsymbol{M}|2\rangle \\ \langle 2|\boldsymbol{M}|1\rangle & \langle 2|\boldsymbol{M}|2\rangle - m \end{vmatrix} = 0 \tag{11}$$

gives the magnetization. Here $\langle i|$ ($|i\rangle$) is the left (right) eigenvector associated with the ith-largest eigenvalue of the transfer matrix. For a given $\widetilde{N}$, the compensation temperature is the temperature below the critical temperature where the magnetization is zero.

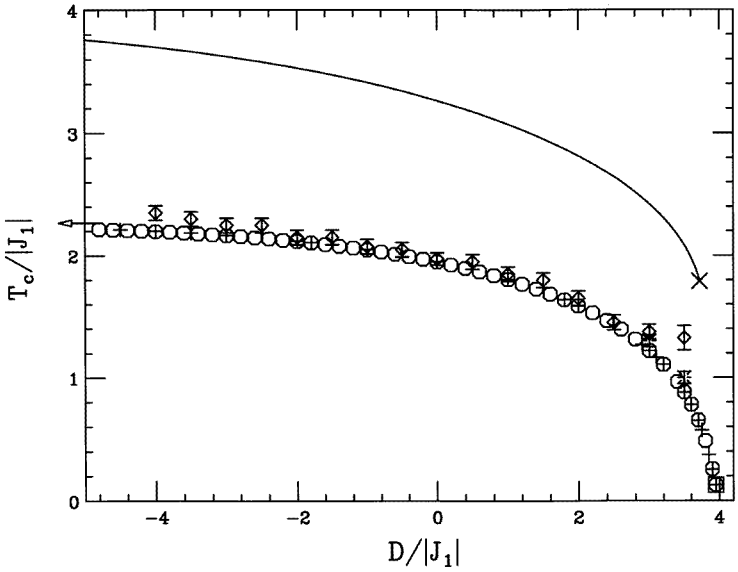

Figure 2. The finite-temperature phase diagram for the $J_4 = 0$ model. The solid line corresponds to the second-order phase transition and its termination at a tricritical point ($\times$) found using a mean-field approximation [16]. The symbols $\Diamond$ ($*$) with error estimates are Monte Carlo results for lattices with $L = 10$ (16). The numerical transfer-matrix (TM1) results are also shown for system sizes $N \times \infty$ and $(N+1) \times \infty$ with $N = 4$ ($\bigcirc$), $N = 6$ ($+$), and $N = 8$ ($\Box$). In the limit $D \to -\infty$, the model reduces to a nn spin-± 1 Ising model, and the arrow indicates the exact value of T_c in this limit.

5. Results

We first tested the mean-field predictions that the $J_4 = 0$ model has a tricritical point and a range of D-values with a compensation point. The ground state for this model corresponds to the line $J_4 = 0$ in figure 1. When $D \to \infty$, one sublattice consists exclusively of $S = 0$ spins, and the magnetic behaviour of the system corresponds to a non-interacting spin-$\sigma = \pm 1$ model arranged on a square lattice. If $D \to -\infty$, the S-spins are never zero, and this limit corresponds to the standard Ising spin-± 1 model on a square lattice with antiferromagnetic ordering. Figure 2 shows the finite-temperature phase diagram for $J_4 = 0$ as a function of $D/|J_1|$ (we choose $J_1 = -1$) obtained with the Monte Carlo and numerical transfer-matrix methods. We also show on the same graph the mean-field results [16]. To get the transfer-matrix results we used TM1 with $N \times \infty$ and $(N+1) \times \infty$ lattices, for $N = 4$, 6, and 8. The Monte Carlo data for the critical temperature were obtained from the location of the specific heat maximum for lattices with $L = 10$ and $L = 16$. These results were confirmed with $L = 40$, but these results are not shown in the figure. As the lattice size increased, the agreement for T_c from the TM and Monte Carlo calculations became closer. The finite-strip-width estimates for y_T calculated with TM1 and TM2 are consistent with the Ising value $y_T = 1$ and are presented in figure 3. Indeed, as N or $\widetilde{N}$ increases, the value for y_T approaches the Ising value for all $D/|J_1| < 4$. These numerical transfer-matrix results strongly suggest that there is a multicritical point only at $T = 0$ located at the point $D/|J_1| = 4$. There is no indication of a tricritical point at finite temperature. Such a tricritical point would be noticeable in that y_T would exhibit a crossover to the thermal exponent associated with a two-dimensional tricritical point, which has $y_T = 1.80$

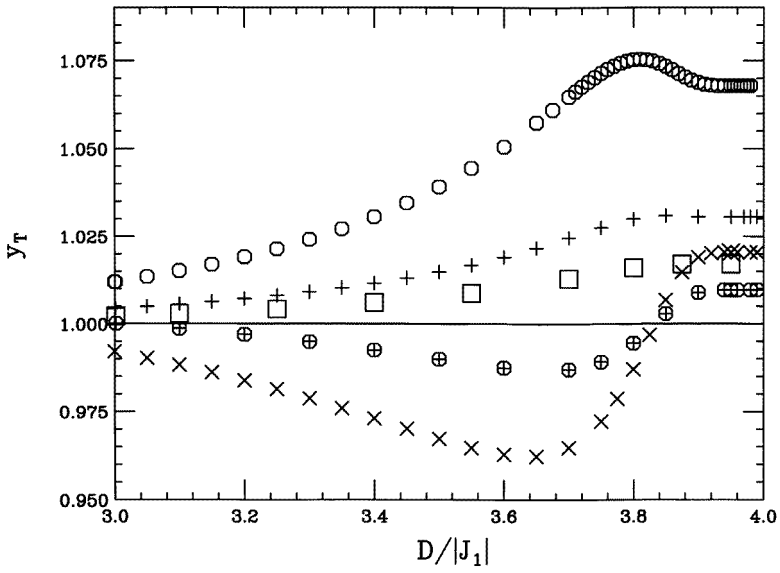

Figure 3. Numerical transfer-matrix results for the critical exponent $y_T = 1/\nu$. Finite-strip-width estimates using $N \times \infty$ and $(N+1) \times \infty$ lattices and TM1 are shown for $N = 4$ (◯), $N = 6$ (+), and $N = 8$ (□). The results obtained from TM2 with $\widetilde{N} \times \infty$ and $(\widetilde{N}+1) \times \infty$ are shown for $\widetilde{N} = 2$ (×) and $\widetilde{N} = 3$ (⊕). It is clear that the results are consistent with the Ising value $y_T = 1$. This becomes more evident as we increase the size.

[30]. Furthermore, past the tricritical point, y_T should approach the value of d associated with a first-order transition. No such crossover is observed. For TM2 there is a change in the direction of approach to $y_T = 1$ as $\widetilde{N}$ becomes larger. However, such behaviour is commonplace, and it is the value of y_T that is converged to which is important, and not the direction of the convergence to this value. It is possible that a tricritical point is located at a much lower temperature that we could study, but even at our lowest value of T_c we do not see any indication of a tricritical point in the behaviour of y_T. An effective-field calculation [17] also has found that $T_c = 0$ for $D/|J_1| \geqslant 4$. Our detailed TM study shows that T_c goes linearly to zero as $T_c/|J_1| = 2.45(\pm 0.11)(4 - D/|J_1|)$ as $D/|J_1| \to 4$. This linear relation holds extremely well between $D/|J_1| \approx 3.8$ and our lowest value of $D/|J_1| = 3.9995$, where we get $T_c/|J_1| = 0.001\,225$. Notice that our results are in excellent agreement with the expected behaviour of the system in the limits of big and small values of D. The magnetization of the $J_4 = 0$ model behaves in the standard way—decreases continuously as the temperature is raised, goes to zero at the critical temperature, and remains zero thereafter—without showing any indication of the presence of a compensation point.

Our non-perturbative results for the $J_4 = 0$ model stand in sharp contrast with the recent studies based on mean- and effective-field theories that indicate that this model has a tricritical point and a compensation point of $D < 4$ [16, 18]. We find no numerical evidence for either of these two phenomena in the $J_4 = 0$ model.

In our search for the type of interaction that must be included to have a compensation point in a mixed Ising ferrimagnetic system, the next step was to include next-nearest-neighbour (nnn) interactions. Adding the nnn interactions between the S-spins, not the J_4-interaction, we found that the finite-temperature phase diagram for the model also showed no evidence of a compensation temperature.

Looking at the zero-temperature phase diagram of the model with nnn interactions J_4 between σ-spins, figure 1, gives us some hope of finding a compensation point for this system. Starting from a ground state in the upper-left-hand quadrant, where the σ-spins are parallel to each other and antiparallel to the S-spins, as the temperature increases the $D > 0$ parameter favours S-spins switching to zero. If, at the same time, there is a strong enough J_4 to oppose the disordering effects of the increasing temperature by keeping the σ-spins parallel to each other, a configuration can be reached where the spin-S sublattice has half of the spins 0, and the other half antiparallel to the σ-spins. For $\sigma = \pm 1$ ($g = 1/2$) spins, this configuration has total magnetization zero but the sublattice magnetizations are not zero. The temperature at which this happens is the compensation temperature.

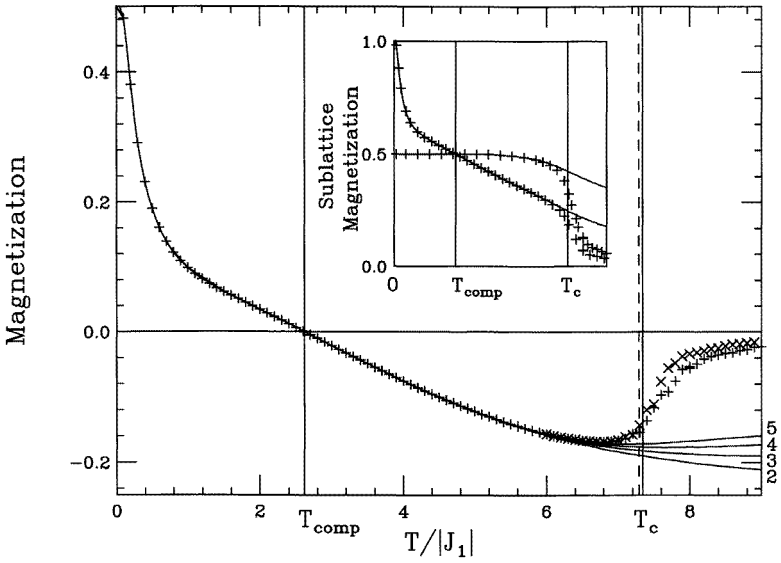

Figure 4. The magnetization versus the temperature for the model at $D/|J_1| = 3.6$ and $J_4/|J_1| = 3$. The distinctive behaviour of the magnetization at the compensation temperature and at the critical temperature can be observed clearly. The results shown are actually those for $|M_1| - (1/2)|M_2|$ for system sizes $L = 40$ (+) and $L = 60$ (×). The ones for $M_1 + (1/2)M_2$ and O_+ are almost identical except close to T_c, where the finite-size effects are largest. The solid curves give the magnetization from equation (11) from the numerical transfer-matrix calculations with $\widetilde{N} = 2$ to $\widetilde{N} = 5$. The numerical TM estimates for T_c from equation (9) are shown as vertical lines for $\widetilde{N} = 2, 3$ (dashed) and $\widetilde{N} = 3, 4$ (solid). In the inset we show the absolute values of the sublattice magnetizations, $|M_1|$ and $|M_2|/2$. Note that $|M_1|$ has the value 1 at $T = 0$. At the compensation point, the two sublattice magnetizations cancel each other. In contrast, at T_c, each one goes independently to zero, except for the remanent finite-size effects.

A general study of the finite-temperature phase diagram for $J_4 \neq 0$ shows that a compensation point exists for a certain range of the J_4-parameter in the region of figure 1 bounded by $J_4/|J_1| > 0$ and $D/|J_1| < 4$. In figure 4 we show an example of the behaviour of the magnetization where the compensation and the critical point can be clearly observed. By analysing the sublattice magnetizations, it is seen that the compensation point appears via the mechanism described above, and that it is due to the different behaviours with temperature of the two sublattices. As the temperature increases, more of the S-spins switch from their ground-state value $+1$ (-1) to 0, but due to the J_4-interaction, more of the σ-spins remain longer in their ground state -1 ($+1$), until, at $T_{\rm comp}$, a configuration (half

of the S-spins are 0, the other half are $+1$ (-1), and the σ-spins remain $+1$ (-1)) is reached where the two sublattice magnetizations cancel each other, giving a total magnetization of zero. If the temperature keeps increasing, $T > T_{\rm comp}$, the absolute values of the sublattice magnetizations decrease but without cancelling each other. The total magnetization increases for a while before it starts to decrease. It will be zero again at the critical temperature where both sublattice magnetizations are zero. For $T > T_{\rm c}$ the magnetizations remain zero.

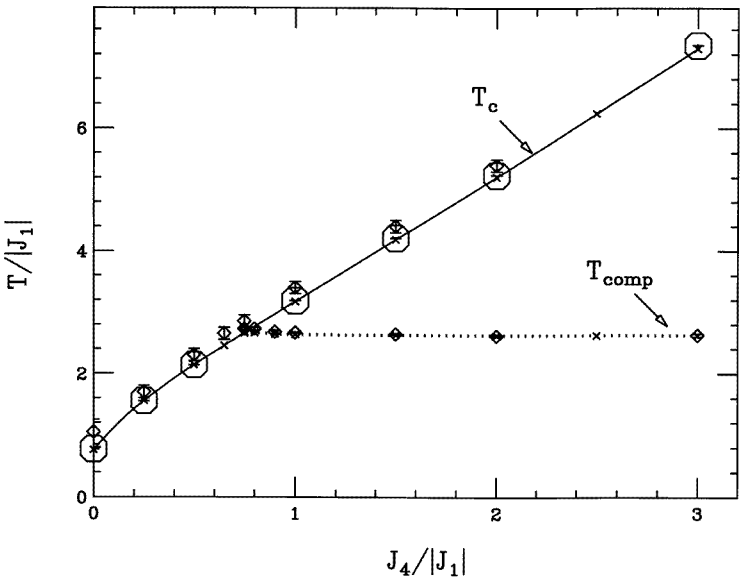

Figure 5. Critical and compensation temperatures, $T_{\rm c}$ and $T_{\rm comp}$, for the model at $D/|J_1| = 3.6$. The critical temperature is shown as a solid line and the compensation temperature as a dotted line. Monte Carlo results for $L = 40$ are shown by the symbol $\diamond$ with error bars. The numerical transfer-matrix (TM2) results for $T_{\rm comp}$ with $\widetilde{N} = 2$ are represented by $\times$. For $T_{\rm c}$, the numerical TM sizes are $\widetilde{N} = 2, 3$ $(\times)$ and $\widetilde{N} = 3, 4$ $(\bigcirc)$. The lines are guides for the eye.

Figure 5 shows the critical and compensation temperatures plotted against J_4 for a particular value of D. The compensation temperature does not exist until the J_4-interaction takes some minimum value, after which it is almost independent of J_4. Notice that $T_{\rm c}$ increases with J_4. This is expected because it is more difficult for the spin lattice to become disordered when there is a strong interaction that tends to keep the σ-spins parallel. The behaviour of $T_{\rm comp}$ is quite different. In order to have a $T_{\rm comp} < T_{\rm c}$, the J_4 must have a minimum value (which depends on D), but once $T_{\rm comp}$ is reached, its value is almost independent of J_4. This behaviour can be explained by looking at figure 4. Increasing J_4 above the minimum value has the effect of keeping the σ-sublattice ordered at higher temperatures, but has no effect on the compensation temperature that was already reached when the S-sublattice magnetization M_1 was equal to $-gM_2$, i.e., at the crossing point of the inset in figure 4.

The compensation temperature, $T_{\rm comp}$, as a function of J_4 and D is shown in figure 6(a). There is a minimum value of J_4 necessary for a compensation point to appear, and it depends on D as is shown in figure 6(a) as a dotted line. Figure 6(b) shows projections of the dotted line in figure 6(a) at which the compensation point first appears as a function of D. The minimum value of J_4 at which a compensation point ($T_{\rm comp} < T_{\rm c}$) appears decreases with increasing values of D. As D increases, the magnetization of the S-sublattice decays faster,

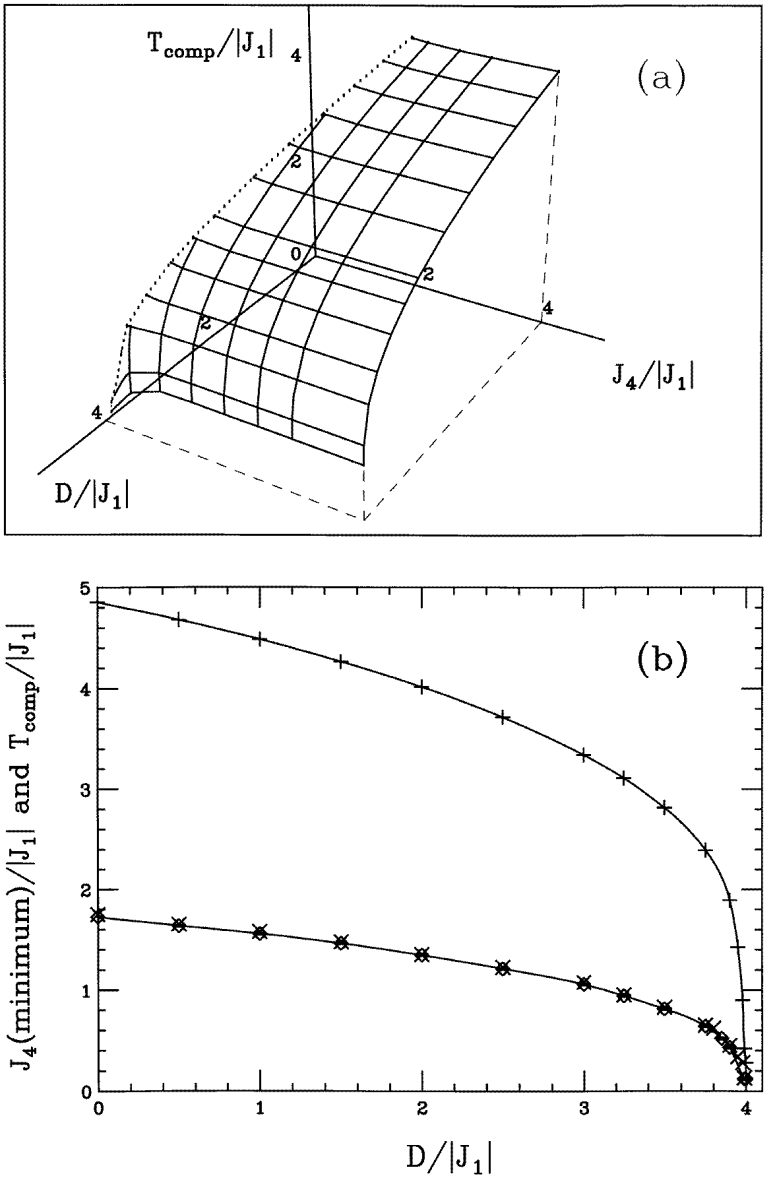

Figure 6. The compensation temperature for the model. (a) was calculated with TM2 and $\widetilde{N} = 2$. The dotted line corresponds to the values below which the compensation point does not exist. (b) Projections of the dotted line in (a), below which the compensation point does not exist: from TM2 and $\widetilde{N} = 2$ the minimum value of J_4 ($\times$) at which a compensation point exists, and the compensation temperature $T_{\rm comp}$ (+) at this minimum value of J_4. Also presented are Monte Carlo results ($\Diamond$) with $L = 40$ for the minimum value of J_4. The solid lines are guides to the eye. Note that J_4(minimum) and $T_{\rm comp}$ seem to go to zero as $D/|J_1| \to 4$.

and the crossing point of the two sublattice magnetizations occurs at a lower temperature, $T_{\rm comp}$, where the σ-sublattice requires only a small value of J_4 to remain ordered. Figure 6 indicates that only at $D/|J_1| = 4$ can there be a compensation point without the nnn

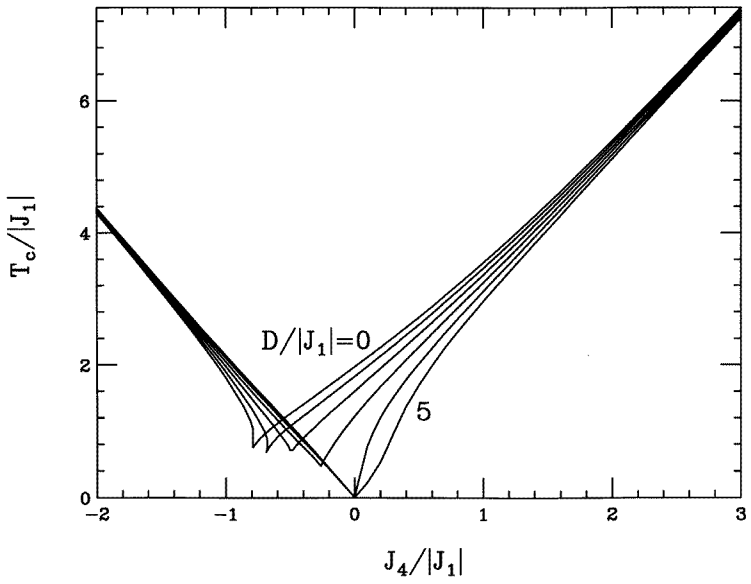

Figure 7. The critical temperature for the model for different values of D. The values were obtained with the numerical transfer-matrix method TM2, with $\widetilde{N} = 2, 3$. The minimum of each graph depends on the values of J_4 and D, but as $|J_4|$ increases, T_c becomes independent of D.

interactions ($J_4 = 0$). However, as one sees in figure 6 and figure 7, both the compensation temperature and T_c go to zero at this point.

The critical temperature calculated using the numerical transfer-matrix method (TM2) is shown in figure 7. The Monte Carlo estimates for T_c obtained from the maximum value of the specific heat are in excellent agreement with the ones obtained with the transfer-matrix method. For large values of J_4, the critical temperature seems to be independent of D, but for small values of J_4, the dependence on D is clearly observed in the graphs. Again, this behaviour is explained by the different temperature dependences of the sublattices. When J_4 is large, the σ-sublattice remains ordered up to quite high temperatures, and this effect dominates the overall behaviour of the model. Our results for T_c are in excellent agreement with the known exact results [20] to which they can be compared. In particular, in figure 7 the exact solution is near the minima of the curves for $D \geqslant 3|J_1$. It is important to emphasize that the exact solution is only known for a two-dimensional manifold in our four-dimensional (T, J_1, J_4, D) space. Furthermore, no portion of the exact solution manifold has $J_4 = 0$, and the exact solution does not provide the sublattice magnetizations.

6. Conclusions

We have applied two non-perturbative methods: Monte Carlo and numerical transfer-matrix calculations, to study a mixed Ising system on a square lattice. The model has two interpenetrating square sublattices, one with spins $\sigma = \pm 1$ and the other with spins $S = \pm 1, 0$. In order to study the ferrimagnetic behaviour of the model, we choose the coupling between nearest neighbours to be antiferromagnetic. We calculated exactly the ground-state phase diagram. Also, we have obtained the finite-temperature phase diagram, and the critical and compensation temperatures for some interesting combinations

of parameters. We found excellent agreement between the Monte Carlo and numerical transfer-matrix data. Since the existence of a compensation point is useful for technological applications such as thermo-optical recording, we consider it important to explore the range and nature of the interactions associated with its existence. Our non-perturbative results are in contradiction with mean- and effective-field studies for the $J_4 = 0$ model (the model with only nn interactions), in which a tricritical point at finite temperatures and a range of D values with a compensation point were found [16, 18]. Consequently, results from methods such as mean- and effective-field predictions for mixed Ising models must be treated with extreme caution. Our results show that a compensation point is induced by the presence of a nnn ferromagnetic interaction, J_4, between the spin-1/2 spins σ. The minimum strength of the nnn interaction $J_4 > 0$ for a compensation point to exist was found to depend on the other parameters of the Hamiltonian. We have demonstrated this in particular for the crystal-field interaction D. We found that the system with only nn interactions does not have a compensation temperature except at the point where the crystal field takes its critical value, $D/|J_1| = 4$, and that the compensation temperature and critical temperature are both zero at this point. On the basis of the above evidence, we conclude that a model with compensation temperature different from zero must have, at least, interactions with non-zero parameters J_1 and J_4. We consider that this result can be of relevance for experimentalists, due to the role of the compensation temperature, as a way to achieve temperature-dependent coercivities. We expect that there may be regions in some experimental two-dimensional ferrimagnets where compensation points may vanish when the couplings between nn and nnn spins are changed, for example by the application of external pressures. Experimental evidence of the effect of long-range interactions on the compensation point can be found in studies involving multilayers with alternating thin layers of pure Tb and Co, where a strong dependence of the compensation temperature on the layer thickness was found [32].

Acknowledgments

Useful discussions with C P Landee, P-A Lindgård, and P A Rikvold are gratefully acknowledged. We also thank J Zhang for checking our exact ground-state calculations for the J_1–D model against his numerical ones. This work was supported in part by the Florida State University, Supercomputer Computations Research Institute, which is partially funded through Contract No DE-FC05-85ER25000 by the US Department of Energy. Also, support from the US DOE grant No DE-FG05-94ER45518 is acknowledged. GMB also acknowledges financial support from the Venezuelan Science Council, CONICIT. MAN is also supported by the National Science Foundation contract No DMR-9520325.

Appendix. Construction of the transfer matrices

This appendix presents the details of the construction of the two implementations, labelled TM1 and TM2, of the transfer matrices that were used in the numerical calculations. We use the notation and methodology of reference [31] to show the form of the TM, and that the TM is symmetric. It is important to realize that in this notation curly brackets denote the matrix product introduced in reference [31].

The first implementation of the TM (TM1) consists of N spins $\sigma = \pm 1$ in the first column and N spins $S = 0, \pm 1$ in the second column. This structure is iterated for an infinite number of columns. This only gives a symmetric matrix if the nnn interactions are zero ($J_4 = 0$). The TM can be written as the symmetric matrix $\mathbf{A}\mathbf{A}^{\mathrm{T}}$. The $2^N \times 3^N$ matrix

$\mathbf{A}$, written for $N = 4$, is explicitly given by

$$\mathbf{A} = \begin{Bmatrix} \mathbf{Q} & \mathbf{Q} & & \\ & \mathbf{Q} & \mathbf{Q} & \\ & & \mathbf{Q} & \mathbf{Q} \\ \mathbf{Q} & & & \mathbf{Q} \end{Bmatrix} \tag{A1}$$

where the 2×3 matrix $\mathbf{Q}$, which takes into account the interaction J_1, is

$$\mathbf{Q} = \begin{pmatrix} \exp[\beta(J_1)] & 1 & \exp[\beta(-J_1)] \\ \exp[\beta(-J_1)] & 1 & \exp[\beta(J_1)] \end{pmatrix}. \tag{A2}$$

In the second TM implementation (TM2), each column contains $\widetilde{N}$ spins σ and $\widetilde{N}$ spins S. The spins are numbered such that in one column a spin σ is the first spin, and in the next column a spin S is the first spin. The TM has the form $\mathbf{D}^{1/2}\mathbf{B}\widetilde{\mathbf{D}}\mathbf{B}^{\mathrm{T}}\mathbf{D}^{1/2}$ where each of the matrices are $6^{\widetilde{N}} \times 6^{\widetilde{N}}$. The matrix $\mathbf{B}$, written for $\widetilde{N} = 3$, has the form

$$\mathbf{B} = \begin{Bmatrix} \mathbf{Q} & \mathbf{S} & & & & \mathbf{S} \\ & \mathbf{Q}^{\mathrm{T}} & & & & \\ & \mathbf{S} & \mathbf{Q} & \mathbf{S} & & \\ & & & \mathbf{Q}^{\mathrm{T}} & & \\ & & & \mathbf{S} & \mathbf{Q} & \mathbf{S} \\ & & & & & \mathbf{Q}^{\mathrm{T}} \end{Bmatrix} \tag{A3}$$

where the 2×3 matrix $\mathbf{Q}$ is given by equation (A2). The 2×2 matrix $\mathbf{S}$ takes into account nnn interactions between spins σ (interaction J_4):

$$\mathbf{S} = \begin{pmatrix} \exp(\beta J_4) & \exp(-\beta J_4) \\ \exp(-\beta J_4) & \exp(\beta J_4) \end{pmatrix}. \tag{A4}$$

The $6^{\widetilde{N}} \times 6^{\widetilde{N}}$ diagonal matrix contains nn interactions between the spins within a column. For $\widetilde{N} = 3$ it is given by

$$\mathbf{D} = \begin{Bmatrix} \mathbf{I}_2 & \mathbf{Q} & & & & \\ & \mathbf{I}_3 & \mathbf{Q}^{\mathrm{T}} & & & \\ & & \mathbf{I}_2 & \mathbf{Q} & & \\ & & & \mathbf{I}_3 & \mathbf{Q}^{\mathrm{T}} & \\ & & & & \mathbf{I}_2 & \mathbf{Q} \\ \mathbf{Q}^{\mathrm{T}} & & & & & \mathbf{I}_3 \end{Bmatrix} \tag{A5}$$

where the matrix $\mathbf{I}_2$ ($\mathbf{I}_3$) is the 2×2 (3×3) identity matrix. The $6^{\widetilde{N}} \times 6^{\widetilde{N}}$ diagonal matrix $\widetilde{\mathbf{D}}$ has the same form as equation (A5), but starts with $\mathbf{I}_3$ rather than $\mathbf{I}_2$ as the first element in the matrix product.

References

[1] Gatteshi D, Kahn O, Miller J S and Palacio F (ed) 1991 *Magnetic Molecular Materials (NATO ASI Series)* (Dordrecht: Kluwer Academic)

[2] Néel L 1948 *Ann. Phys., Paris* **3** 137

[3] Szpunar B and Lindgård P-A 1977 *Phys. Status Solidi* b **82** 449

[4] For a theoretical study, see
Curely J, Georges R, Drillon M, Belaiche M and Benkhouja K 1992 *Phys. Rev.* B **46** 3527

[5] Kahn O, Pei Y, Verdaguer M, Renard J P and Sletten J 1988 *J. Am. Chem. Soc.* **110** 782
Caneschi A, Gatteshi D, Sessoli R and Rey P 1989 *Mol. Cryst. Liq. Cryst.* **176** 329

[6] Willet R D, Wang Z, Molnar S, Brewer K, Landee C P, Turnbull M M and Zhang W 1993 *Mol. Cryst. Liq. Cryst.* **233** 277

[7] Tamaki H, Zhong Z J, Matsumoto N, Kida S, Koikawa M, Achiwa N, Hashimoto Y and Okawa H 1992 *J. Am. Chem. Soc.* **114** 6974
Okawa H, Matsumoto N, Tamaki H and Ohba M 1993 *Mol. Cryst. Liq. Cryst.* **233** 257
[8] Turnbull M M, Landee C P, Soesbe T C and Willett R D 1993 *Mol. Cryst. Liq. Cryst.* **233** 269
[9] Decurtins S, Schmalle H W, Oswald H R, Linden A, Ensling J, Gütlich P and Hauser A 1994 *Inorg. Chim. Acta* **65** 216
[10] Mallah T, Tiebaut S, Verdaguer M and Veillet P 1993 *Science* **262** 1554
[11] Du G, Joo J and Epstein A J 1993 *J. Appl. Phys.* **73** 6566
Manriquez J, Lee G T, Scott R, Epstein A and Miller J 1991 *Science* **252** 1415
[12] Mathonière C, Nuttall C J, Carling S G and Day P 1996 *Inorg. Chem.* **35** 1201
[13] Hunter G J A, Jenkins R C L and Tinsley C J 1990 *J. Phys. A: Math. Gen.* **23** 4547
Bowers R G and Yousif B Y 1983 *Phys. Lett.* **96A** 49
[14] Schofield S L and Bowers R G 1980 *J. Phys. A: Math. Gen.* **13** 3697
[15] Quadros S G A and Salinas S R 1994 *Physica* A **206** 479
[16] Kaneyoshi T and Chen J C 1991 *J. Magn. Magn. Mater.* **98** 201
[17] Siqueira A F and Fittipaldi I P 1986 *J. Magn. Magn. Mater.* **54–57** 678
[18] Kaneyoshi T 1989 *Solid State Commun.* **70** 975
[19] Bobák A and Jaščur M 1995 *Phys. Rev.* B **51** 11 533
[20] Lipowski A and Horiguchi T 1995 *J. Phys. A: Math. Gen.* **29** L261
[21] Mansuripur M 1987 *J. Appl. Phys.* **61** 1580
[22] Shieh Han-Ping D and Kryder M H 1986 *Appl. Phys. Lett.* **49** 473
[23] Buendía G, Novotny M A and Zhang J 1994 *Computer Simulations in Condensed Matter Physics VII* ed D P Landau, K K Mon and H B Schüttler (Berlin: Springer) p 223
[24] Herpin A 1968 *Théorie du Magnétism* (Paris: Press Universitaires de France)
[25] Karl G 1973 *Phys. Rev.* B **7** 2050
Schick M 1982 *Prog. Surf. Sci.* **11** 245
[26] Binder K 1979 *Monte Carlo Methods in Statistical Physics* ed K Binder (Berlin: Springer)
[27] Marsaglia G and Zaman A, unpublished
[28] Nightingale M P 1990 *Finite Size Scaling and Numerical Simulation of Statistical Systems* ed V Privman (Singapore: World Scientific)
[29] Bartelt N C, Einstein T L and Roelofs L D 1986 *Phys. Rev.* B **34** 1616
[30] Landau D P and Swendsen R H 1981 *Phys. Rev. Lett.* **46** 1437
[31] Novotny M A 1978 *J. Math. Phys.* **20** 1146
Novotny M A 1988 *J. Math. Phys.* **29** 2280
[32] Ertl L, Endl G and Hoffmann H 1992 *J. Magn. Magn. Mater.* **113** 227